NANO LETTERS

Letter

Cite This: Nano Lett. 2019, 19, 4787−4796

pubs.acs.org/NanoLett

Unraveling the Macromolecular Pathways of IgG Oligomerization and Complement Activation on Antigenic Surfaces

Jürgen Strasser,[†] Rob N. de Jong,[‡] Frank J. Beurskens,[‡] Guanbo Wang,[§,∥,⊥] Albert J. R. Heck,[§,⊥] Janine Schuurman,[‡] Paul W. H. I. Parren,[#,▽] Peter Hinterdorfer,[○] and Johannes Preiner*[,†]

[†]University of Applied Sciences Upper Austria, 4020 Linz, Austria

[‡]Genmab, 3584 CM Utrecht, The Netherlands

[§]Biomolecular Mass Spectrometry and Proteomics, Bijvoet Center for Biomolecular Research and Utrecht Institute for Pharmaceutical Sciences, Utrecht University, Padualaan 8, 3584 CH Utrecht, The Netherlands

[∥]School of Chemistry and Materials Science, Nanjing Normal University, 1 Wenyuan Road, Nanjing 210023, China

[⊥]Netherlands Proteomics Centre, Padualaan 8, 3584 CH Utrecht, The Netherlands

[#]Department of Immunohematology and Blood Transfusion, Leiden University Medical Center, 2333 ZA Leiden, The Netherlands

[▽]Lava Therapeutics, 3584 CM Utrecht, The Netherlands

[○]Johannes Kepler University Linz, 4020 Linz, Austria

Supporting Information

ABSTRACT: IgG antibodies play a central role in protection against pathogens by their ability to alert and activate the innate immune system. Here, we show that IgGs assemble into oligomers on antigenic surfaces through an ordered, Fc domain-mediated process that can be modulated by protein engineering. Using high-speed atomic force microscopy, we unraveled the molecular events of IgG oligomer formation on surfaces. IgG molecules were recruited from solution although assembly of monovalently binding molecules also occurred through lateral diffusion. Monomers were observed to assemble into hexamers with all intermediates detected, but in which only hexamers bound C1. Functional characterization of oligomers on cells also demonstrated that C1 binding to IgG hexamers was a prerequisite for maximal activation, whereas tetramers, trimers, and dimers were mostly inactive. We present a dynamic IgG oligomerization model, which provides a framework for exploiting the macromolecular assembly of IgGs on surfaces for tool, immunotherapy, and vaccine design.

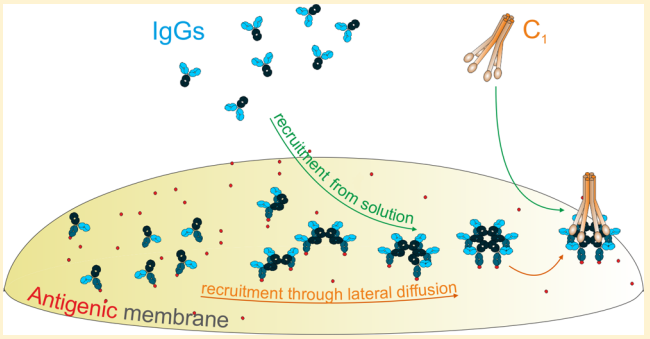

KEYWORDS: *IgG hexamers, IgG oligomerization, classical complement pathway, C1, immune complex formation, high-speed atomic force microscopy, native mass spectrometry*

Elimination of antibody-opsonized cells is mediated by different branches of the innate immune system—powerful natural defense mediators that are increasingly utilized in immunotherapy to eliminate infectious agents, regulatory immune cells, or cancer cells. These mediators include the classical complement pathway, composed of an amplifiable cascade of soluble zymogens that is present in blood and other biological fluids and immune effector cells such as NK cells, monocytes, and neutrophils. Activation of complement is an important step in alerting and triggering immune protection since it occurs almost instantaneously upon contact with antibody−antigen complexes thereby producing an abundance of chemoattractants and opsonins that serve to attract and activate immune effector cells. Uncontrolled or exaggerated complement activation furthermore plays a role in the pathogenicity of certain autoimmune or inflammatory diseases and may result in (first dose) toxicity observed after therapeutic antibody treatment. The ability and potency of monoclonal antibodies (mAbs) to induce complement activation are dependent on various factors, such as IgG isotype and the physiochemical properties of antigen and epitope recognized.[1−7] The classical pathway of complement is initiated by the interaction of multimerized IgG with complement factor C1, consisting of one (hexameric) C1q subunit and a heterotetramer consisting of a doublet of the zymogens C1r and C1s. Although C1 has been structurally characterized in complex with IgG, it is currently still uncertain what signals trigger its initial activation.[8,9]

Received: May 31, 2019
Revised: June 5, 2019
Published: June 6, 2019

DOI: 10.1021/acs.nanolett.9b02220
Nano Lett. 2019, 19, 4787−4796

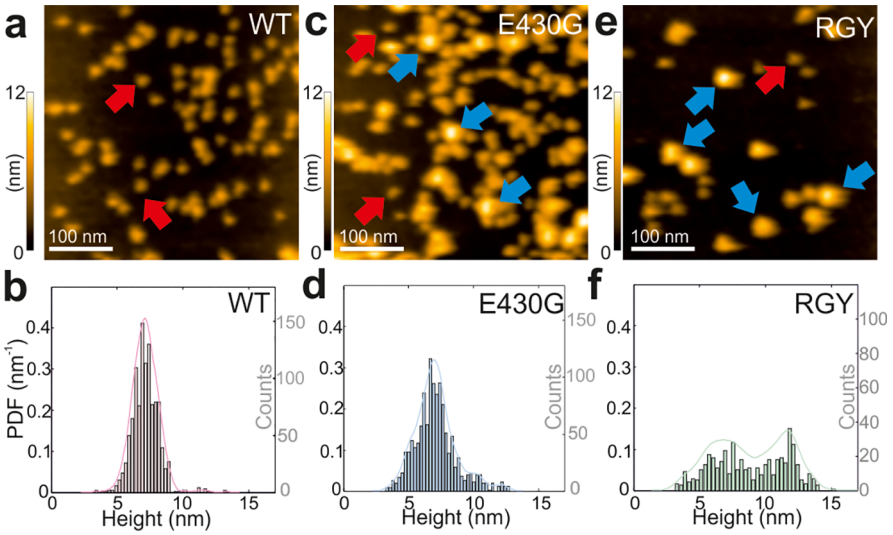

Figure 1. HS-AFM imaging of wild-type IgG1 and hexamerization-enhanced mutants bound to DNP antigen-containing supported lipid bilayers (SLBs). First frame of HS-AFM overview scans of IgG1-DNP-WT (a), IgG1-DNP-E430G (c), and IgG1-DNP-RGY (e) bound to DNP-SLBs. More frames of the same movies (Movies S1−S3) are displayed in the Supporting Information, Figure S1c−e, respectively. Arrows indicate IgG monomers (red) or hexamers (blue). Height distributions presented as probability density functions (PDFs, left) with corresponding histograms (Counts, right) of IgG1-DNP-WT (b; n = 1096), IgG1-DNP-E430G (d; n = 1221), and IgG1-DNP-RGY (f; n = 481) compiled from the respective overview scans.

Multiple IgG molecules are required for C1 activation, since the binding affinity of C1 for monomeric IgG is very low (~10^{-4} M). Whereas early studies suggested IgG dimers to be sufficient, others demonstrated that C1 binding strength and activation increased with IgG aggregate size and antigen density, indicating that higher-order multimers are required.[10−17] Recent studies have shown that C1 is strongly activated by ordered IgG hexamers consisting of six IgG molecules that interact through a relatively large interface of noncovalent Fc−Fc interactions.[18] The fraction of IgG molecules existing in hexamers at the cell surface or in solution and the potency of complement activation could be increased or decreased by specific point mutations at the Fc−Fc interface.[18,19] Despite all progress, the mechanism of assembly of IgG into oligomers and IgG−C1 complexes, the dynamics and kinetics of these interactions, as well as the ability of intermediates to productively interact and activate complement remain largely unknown. Here, we set out to describe the biophysical and structural characteristics of C1—immune complex formation in detail from (i) the initial recognition of antigenic membranes by IgG molecules to (ii) the stepwise assembly of antibody oligomer intermediates into hexamers and (iii) the macromolecular requirements of C1 binding and activation. Recent developments in high-speed atomic force microscopy[20] (HS-AFM) that lead to the dynamic visualization of motor proteins,[21,22] membrane proteins,[23−26] and cells[27−29] enabled us to visualize these processes at submolecular resolution and in real time. Functional experiments complemented by native mass spectrometry were performed to characterize the stereochemical requirements of multivalent C1q binding sites within IgG oligomers that lead to C1 activation on tumor cells.

Fc Mutations Modulate IgG Oligomerization. As a model for an antigenic membrane, we used a supported lipid bilayer (SLB)containing dinitrophenyl (DNP)-labeled lipids, generated on a mica surface by vesicle fusion (DNP-SLBs; Supporting Information, Figure S1a). Incubation of this membrane with wild-type chimeric human IgG1 anti-DNP mAb (IgG1-DNP-WT; Supporting Information, Figure S1b) resulted in a sparse distribution of mainly isolated bivalently bound IgGs with heights of ~6−7 nm[30] as observed by HS-AFM (Figure 1a, red arrows; Supporting Information, Figure S1c, Movie S1). Only a minor fraction of higher-order antibody assemblies (~12 nm in size, Figure 1b) were observed under these conditions. The single point mutant IgG1-DNP-E430G (E430G), which was previously shown to display enhanced complement-dependent cytotoxicity (CDC) of cells,[19,31] was demonstrated to exist in increased populations of higher-order IgG1-E430G antibody assemblies on DNP-SLB membranes (Figure 1c, blue arrows; Supporting Information, Figure S1d, Movie S2; height distribution, Figure 1d).

The triple mutant IgG1-DNP-RGY (IgG1-E345R, E430G, and S440Y), which was shown to efficiently associate into IgG1 hexamers in solution,[18,31] exhibited the largest fraction (approximately 50%) of such larger IgG assemblies (Figure 1e,f; Supporting Information, Figure S1e, Movie S3). The binding and oligomerization of IgG1-DNP-WT, IgG1-E430G, and IgG1-RGY on DNP-SLBs were specific, as incubation of the irrelevant isotype control antibody IgG1-b12 resulted in flat, featureless membranes (Supporting Information, Figure S1f). We then developed a special HS-AFM imaging protocol to determine the oligomeric state of the antibody assemblies, i.e., the number of IgG monomers per oligomer. HS-AFM imaging at set-point amplitudes close to the free amplitude of the cantilever oscillation (90−95%) keeps the imaging forces low enough to obtain images of individual IgG oligomers (Figure 2a). Intentionally decreasing the set-point amplitude (thus increasing the effective imaging force) induced the dissociation of IgG oligomers in a controlled manner and could thus be used to identify objects as monomers, dimers, trimers, tetramers, pentamers, and hexamers on the basis of their dissociation pattern (Figure 2b; Movies S4 and S5). This allowed us to unequivocally classify the observed assemblies with respect to their dimension and shape as oligomers containing different multiples of IgGs as shown. Notably, no

DOI: 10.1021/acs.nanolett.9b02220
Nano Lett. 2019, 19, 4787−4796

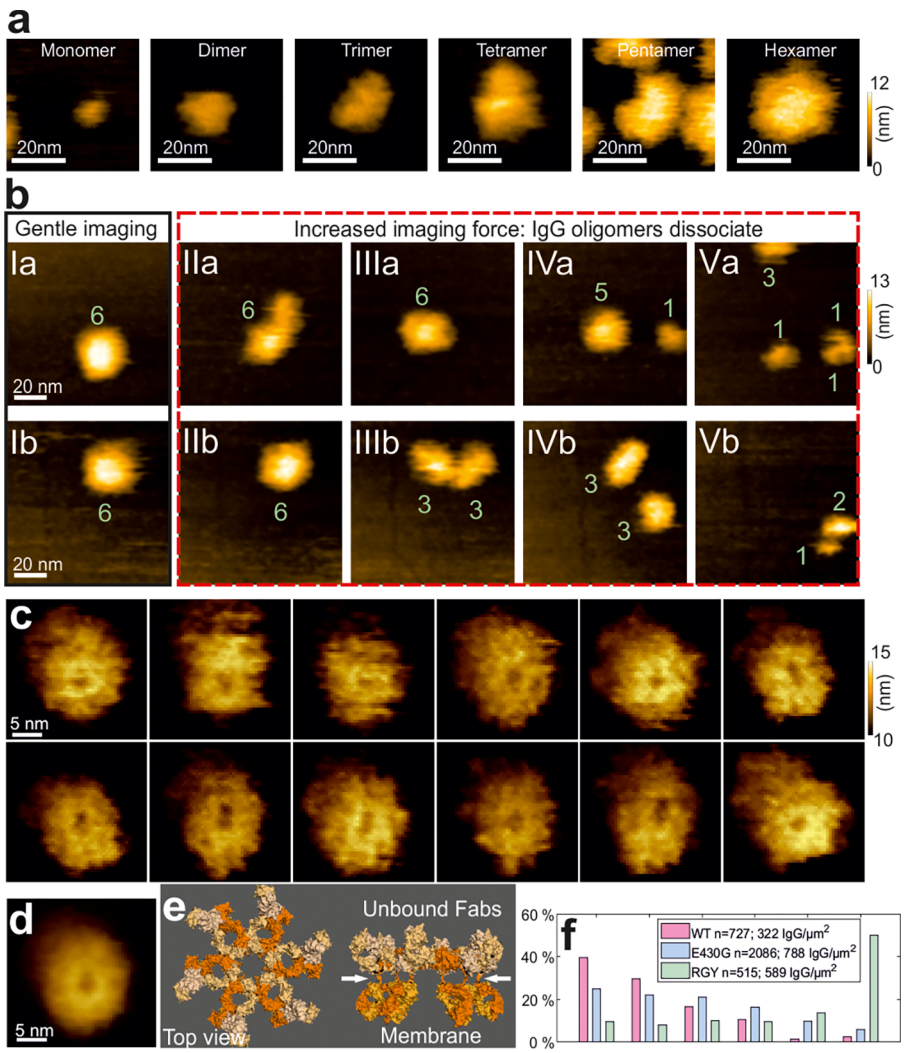

Figure 2. IgG oligomers on DNP antigen-containing supported SLBs. (a) High-resolution images of observed IgG oligomer classes. (b) Force-induced dissociation of IgG oligomers. Ia: intact IgG1-DNP-RGY hexamer. IIa: increasing the scanning force first results in loss of internal coherence; i.e., one or more Fc−Fc bonds are broken but still might reform. IIIa: the six IgGs are still connected and have congregated once more. IVa: a small object (likely a monomer) breaks off from the main complex (but remains bound to the DNP-SLB). Va: dissociation continues. Four subcomplexes have formed, likely three monomers and a trimer. Full sequence: Movie S4. Ib: intact IgG1-DNP-RGY hexamer. IIb: the hexamer is deformed upon application of an increased force. IIIb−IVb: the hexamer splits into two trimeric halves. Vb: eventually they dissociate. Full sequence: Movie S5. (c) High-resolution images of an IgG hexamer exhibiting internal structural features selected from Movie S6. (d) The average of the images depicted in part c reveals a platform resembling the Fc arrangement including the central hole. (e) Model of the antigenic membrane-bound IgG hexamer[18] based on the IgG1-b12 crystal structure.[32] The arrows depict the parts of the IgG heavy chains within the flexible hinge regions that connects the Fc platform with the membrane-bound Fab fragments. (f) Comparison of oligomer abundance for IgG1-DNP-WT (WT, pink), IgG1-DNP-E430G (E430G, blue), and IgG1-DNP-RGY (RGY, green). The histogram displays the fraction of IgGs constituting the respective oligomer species.

oligomers larger than hexamers were observed. Even though being very flexible and only punctually (through six Fab fragments) attached to the membrane surface, we were able to resolve the hexamer's Fc platform[9,18,32] including the most prominent central hole (Figure 2c taken from Movie S6; average image, Figure 2d). The topographical variation within the images provides evidence for the overall flexibility of the structure (Figure 2e) that is largely caused by the loose linkage between the Fc platform and the surface-bound Fabs through the flexible IgG hinge regions (Figure 2e, arrows) as well as through a diffuse halo constituting the flexible, surface-unbound Fab arms. We deduced histograms of the oligomer distributions for each IgG variant from the HS-AFM recordings (Figure 2f). The distributions were shifted toward higher-order oligomers for both the IgG1-E430G and IgG1-RGY mutant when compared to wild-type (WT), with as expected IgG1-RGY showing the highest hexamer abundance. The increased distribution of the E430G and RGY mutants into higher-order oligomers is consistent with their increased potency in complement activation (Supporting Information, Figure S2).

Two Distinct Pathways Contribute to IgG Oligomerization. IgG oligomerization on antigenic membranes may proceed via two possible pathways. First, IgG molecules may bind to mobile DNP antigens, collide, and oligomerize through Fc−Fc interactions. We termed this process of 2D diffusion-based oligomerization the "lateral pathway". Alternatively, antigen-bound IgG may recruit additional IgG molecules into the oligomer from solution via Fc−Fc interactions. We describe this process as the "vertical pathway". The HS-AFM

DOI: 10.1021/acs.nanolett.9b02220
Nano Lett. 2019, 19, 4787−4796

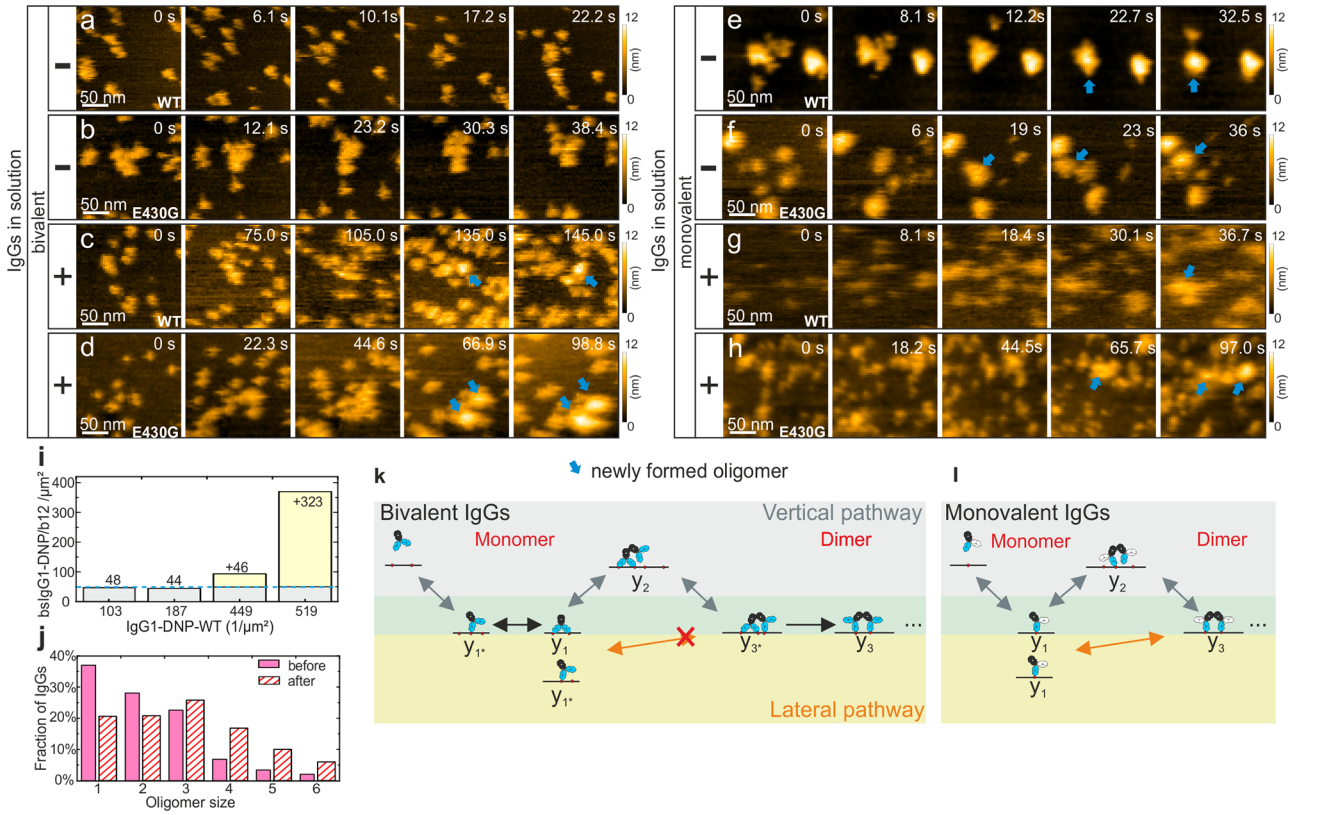

Figure 3. Mechanism of IgG oligomerization. (a), (b) Time series of IgG1-DNP-WT (a) and IgG1-DNP-E430G (b; Movie S7) bound to DNP-SLB incubated in the absence of the respective solution-phase antibody. Oligomerization of colliding IgGs was not observed. (c), (d) Time series as in panels a and b, but in the presence of solution-phase IgG1-DNP-WT (c) or IgG1-DNP-E430G (d; Movie S8). The formation of IgG oligomers through recruitment from solution can be observed as indicated by blue arrows. (e), (f) Time series of the functionally monovalent bsIgG1-DNP/b12 (e) and bsIgG1-DNP/b12-E430G (f; Movie S9) bound to a DNP-SLB in the absence of the respective solution-phase antibody. In contrast to bivalent IgGs, oligomerization via lateral collisions is observed. (g), (h) Time series as in panels e and f, but in the presence of solution-phase monovalent bsIgG1-DNP/b12 (g) or bsIgG1-DNP/b12-E430G (h; Movie S10). (i) bsIgG1-DNP/b12 recruitment to DNP-SLBs decorated with defined IgG1-DNP-WT densities. The dashed blue line represents the bsIgG1-DNP/b12 density obtained on bare DNP-SLBs. (j) Comparison of oligomer abundances before and after addition of bsIgG1-DNP/b12 to 519 IgG1-DNP-WTs/μm^2. (k) Dynamic model of IgG oligomerization at high epitope density (single IgGs predominantly exist in the bivalently bound state). An IgG initially binds monovalently to a surface epitope (y_{1*}) from solution, immediately followed by bivalent attachment. Bivalently attached IgGs (y_1) may serve as nucleation sites for oligomerization through recruitment from solution (y_2 to y_{3*}, vertical pathway), whereas lateral collisions (lateral pathway) between IgGs do not significantly contribute (y_{1*} to y_3). (l) Monovalently bound IgGs have access to an additional pathway. After initial attachment (y_1), oligomerization continues either via recruitment from solution (y_2) or via lateral collisions ($y_1 \times y_1$) leading to dimers (y_3) and through repetition of either pathway to higher-order oligomers.

data presented thus far were recorded in IgG-free buffer. Bivalent IgG molecules bound to DNP-labeled lipids were found to display moderate mobility resulting in occasional lateral collisions, which however did not result in oligomer formation (Figure 3a,b; Movie S7). For both IgG1-WT and IgG1-E430G, bivalent attachment to membrane epitopes therefore appeared to sterically suppress Fc−Fc interactions between colliding IgGs, essentially excluding the lateral pathway as a means to generate the IgG distributions observed in Figure 2f. Oligomerization through the vertical pathway, on the other hand, became apparent once IgG was added to the surrounding solution (Figure 3c,d; Movie S8). In real-time measurements, we first observed individual IgG molecules decorating the membrane, after which small oligomers appeared that finally grew into hexamers (within ~100/140 s for E430G and WT). The vertical pathway thus enables the formation of the observed oligomer populations, and the E430G mutation directly impacts the efficiency of this pathway (Figure 2f). Interestingly, oligomerization through the lateral pathway was observed for IgG1 molecules that can only bind the DNP antigen monovalently. To obtain (functionally) monovalent IgG1 molecules, we generated bispecific (bs)IgGs in which one of the DNP-binding Fab arms was exchanged with a Fab arm (b12) against an irrelevant control antigen. Both bsIgG1-DNP/b12 and bsIgG1-DNP/b12-E430G assembled into oligomers through lateral collision (in the absence of any solution-phase IgG) during imaging (Figure 3e,f; Movie S9). Therefore, monovalent bsIgGs are capable of oligomerizing through either the vertical (Figure 3g,h; Movie S10) or the lateral (Figure 3e,f; Movie S9) pathway.

We then investigated the interplay between IgG molecules with monovalent and bivalent binding capabilities. Bivalent IgGs are able to bind at higher density (Supporting Information, Figure S3a,b) and create greater absolute oligomer abundance (Figure 2f versus Supporting Information, Figure S3c) than monovalent bsIgGs. Complement activation assays on DNP-labeled liposomes followed a similar trend with a 10−100 fold higher potency of bivalent IgGs compared to the equivalent monovalent bsIgG (Supporting Information, Figure S2). To assess the role of the nucleating

DOI: 10.1021/acs.nanolett.9b02220
Nano Lett. 2019, 19, 4787−4796

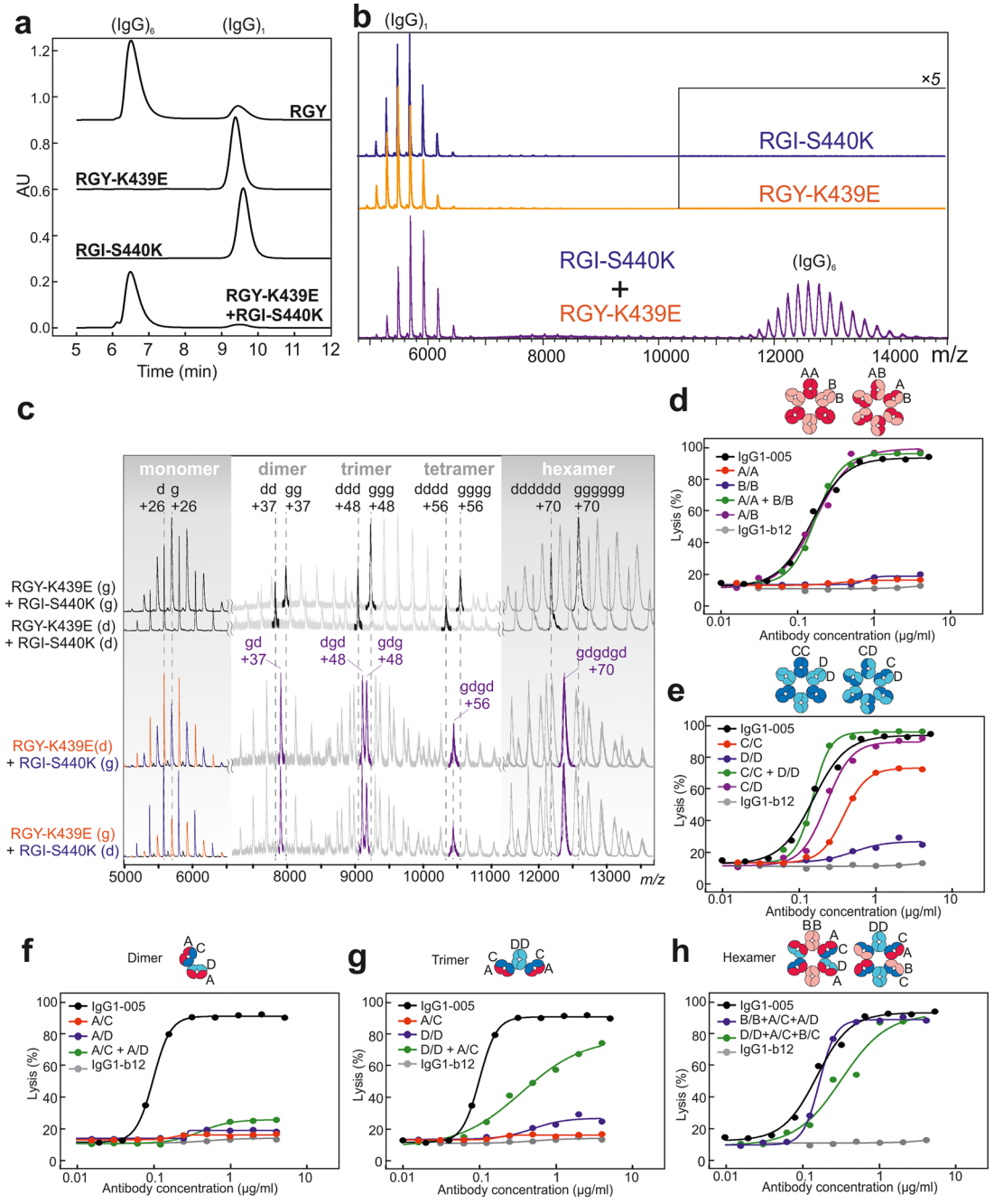

Figure 4. Complement activation by IgG oligomers of different sizes. (a) HP-SEC chromatograms of IgG1-005 variants and a 1:1 mixture of RGY-K439E+RGI-S440 K, staggered at 0.3 AU per trace along the *y*-axis (absorption; arbitrary units). *x*-axis: elution time (min). (b) Native MS spectra of IgG1 variants described under part a. *x*-axis, *m*/*z* ratio; *y*-axis, signal intensity. Signal intensity in the high-*m*/*z* section of spectra was amplified 5-fold for RGY-K439E and RGI-S440 K relative to the 1:1 mixture thereof. (c) Native MS spectra as under part b of IgG1 hexamers assembled in 1:1 mixtures of RGY-K439E and RGI-S440 K, composed of glycosylated (*g*) and/or deglycosylated (*d*) components to allow identification of the component by their molecular weight. Numbers indicated at the top of the spectra indicate charge states. Signal intensities were normalized to the highest peak per section (monomer, trimer, hexamer) to facilitate visualization. (d–h) CDC of Daudi cells opsonized with a concentration range (*x*-axis) of different IgG1-005 variants, detailed in the Supporting Information, Table S1, and mixtures thereof. Cell lysis was assessed with flow cytometry by using propidium iodide staining. Note that mutant C in panel e is strongly reduced in CDC but not fully inhibited, potentially resulting in C/C-mediated dimers in panels f and g. Wild-type IgG-005 is used as a positive and the irrelevant IgG1-b12 as a negative control.

(bivalently bound) IgG in oligomerization through the vertical pathway, we prepared four different IgG1-DNP-WT densities (ranging from 103 to 519/μm^2) on DNP-SLBs and exposed them to monovalent bsIgG1-DNP/b12 under conditions that generated ~50 bsIgG1-DNP/b12 molecules/μm^2 on bare DNP-SLBs (Supporting Information, Figure S3c). Figure 3i shows that, at low IgG1-DNP-WT densities, the additional binding was negligible; however, at the higher densities, bsIgG1-DNP/b12 was more efficiently recruited (7.4-fold at 519 IgG1-DNP-WT/μm^2), and the resulting IgG distribution was shifted toward higher-order oligomers (Figure 3j). Notably, the remaining fraction of monomers was significantly lowered, suggesting that IgG1-DNP-WT served as an effective nucleation site for IgG oligomerization.

DOI: 10.1021/acs.nanolett.9b02220
Nano Lett. 2019, 19, 4787–4796

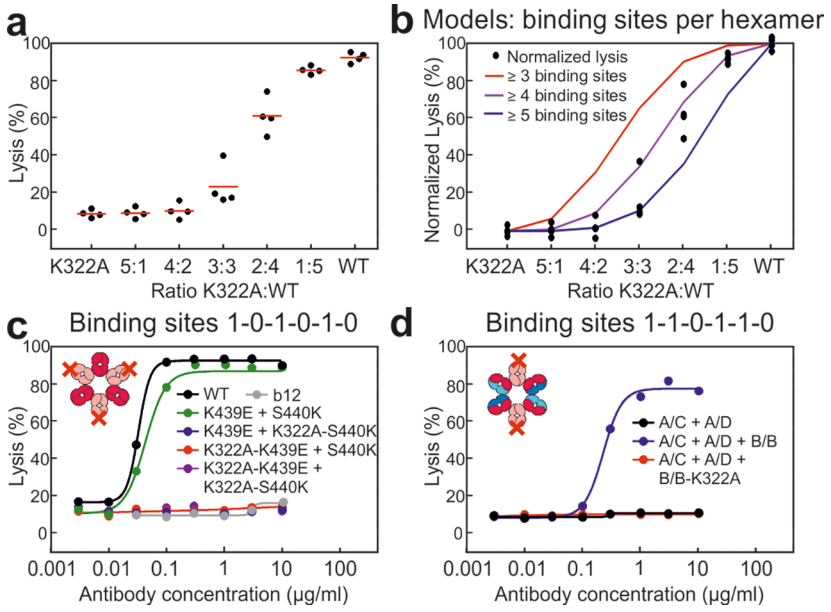

Figure 5. Valency of the C1q binding site in IgG required for complement activation. (a) Lysis observed at saturating antigen binding during CDC of Daudi cells opsonized with IgG1-005-K322A, IgG1-005, and different mixtures thereof. (b) Maximal lysis values observed under part a normalized relative to maximal lysis induced by IgG1-005 (100%) and IgG1-005-K322A (0%), fitted to stochastic probability distributions of different numbers of wild-type C1q binding sites per IgG hexamer as a function of the IgG1-005-K322A:IgG1-005 ratio. (c, d) CDC of Daudi cells. Lysis was assessed with flow cytometry by using propidium iodide staining. Daudi cells were either opsonized with IgG variants with regular C1q binding sites or with IgG hexamers in which C1q binding sites were knocked out using K322A mutations either in alternating fashion (c) or at two opposing sites (d).

Mechanism of IgG1 Oligomerization. On the basis of our data, we can discriminate two potential oligomerization scenarios. First, on surfaces with high antigen density (Figure 3k), an IgG initially binds monovalently to a surface epitope from solution, followed by bivalent attachment. Additional IgGs are recruited through Fc−Fc interactions to the vicinity of the membrane enabling the formation of an additional epitope−paratope bond, resulting in a "tripod" arrangement. After the release of one epitope−paratope bond, an IgG dimer amenable to recruit additional IgGs is realized. Then, oligomerization continues through the Fc-mediated binding of additional IgGs out of solution that may bind to any of the two unoccupied Fc domains in the respective oligomer. Oligomerization through lateral collisions is unlikely, as high epitope densities virtually preclude single IgGs from being monovalently bound for a sufficiently long time, and bivalently bound IgGs do not follow this pathway (Figure 3a,b). Second, on surfaces with low antigen density or, alternatively, in the presence of high IgG concentrations in solution, IgGs are predominantly monovalently bound (Figure 3l), and therefore oligomerization may occur via both pathways, i.e., recruitment from solution (vertical pathway) and 2D collisions (lateral pathway).

IgG Dimers and Trimers Fail To Induce Efficient CDC Activation. We observed a distribution of IgG oligomers of different sizes on DNP-labeled lipid bilayers (Figures 2 and 3), which raised the question of which intermediates might be active in complement activation. To test which IgG oligomer sizes can activate C1 on cells, we set out to assemble oligomers of defined sizes on cell surfaces. We therefore created IgG molecules with Fc domains that were mutated to inhibit intermolecular Fc−Fc interactions using previously identified complementary mutations (e.g., of opposite charge).[18,33] These mutations are in close proximity in the Fc−Fc interface and therefore prevent homologous Fc−Fc pairing, whereas oligomerization of (alternating) heterologous Fcs is unaffected (Supporting Information, Figure S4). Several mutants were produced containing either complementary mutations A (K439E) and B (S440 K) or complementary mutations C (C-terminal-PGE) and D (C-terminal-PGKKP). We have previously shown that mutant A can only form a stable Fc−Fc interface with B and similarly C with D, but not with itself.[18,33] Antibodies with asymmetric Fc domains combining different mutations in their two heavy chains were prepared by generating bispecific IgGs in a procedure which allows the controlled exchange of a heavy chain−light chain pair between IgG antibodies.[34] The availability of these distinct "building blocks" allowed us to generate IgG monomers, dimers, trimers, and hexamers on cells (Supporting Information, Figure S4).

To biophysically verify our molecular design, we assessed the effect of introducing mutations K439E or S440 K into two IgG1 triple mutants that showed spontaneous oligomerization in solution and therefore were amenable to size exclusion (HP-SEC) and native mass spectrometry (MS) analysis. We included the RGY mutation discussed above and used a second triple mutant termed RGI (E345R-E430G-Y436I).[31] HP-SEC and MS analyses demonstrated that both RGY-K439E (i.e., containing mutation A) and RGI-S440 K (i.e., containing mutation B) indeed were self-inhibited and retained their monomericity. Upon mixing, however, heterohexameric complexes were formed (Figure 4a,b). To allow (increased) discrimination of the two antibodies in the various assemblies, deglycosylated IgGs were generated (Figure 4c) enabling us to mass resolve the subunits present in the higher-order oligomers. The native MS data revealed that dimeric complexes exclusively contained one K439E- and one S440 K-derived variant ("gd") and never two of the same mutants, demonstrating strict alternating assembly. Trimeric complexes

DOI: 10.1021/acs.nanolett.9b02220
Nano Lett. 2019, 19, 4787−4796

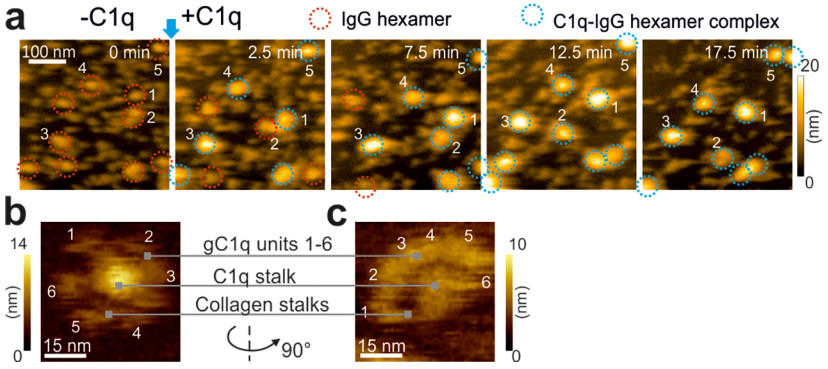

Figure 6. C1q exclusively binds to higher-order IgG oligomers. (a) HS-AFM time series demonstrating direct C1q binding to IgG1-DNP-E430G hexamers. After localization of potential hexamers, C1q was added to the sample, and binding was followed over time (some of the individual hexamers/complexes are labeled (1−5) throughout the image sequence to follow them over time). (b) HS-AFM image of a single C1q molecule recorded on bare mica (taken from Movie S11). Six flexible globular gC1q units surround a central stalk exhibiting a height of 10.6 ± 1.9 nm. (c) Same C1q molecule as in part b flipped sideways.

were always in a two plus one configuration ("dgd" or "gdg"), while tetrameric and hexameric variants always contained equal amounts of both the A and B mutant. We concluded that these two mutations direct the assembly of heterohexameric rings in strictly alternating order, consistent with our molecular design.

We then studied the ability of the original mutant panel (i.e., only containing various combinations of mutations A, B, C, and D) to induce complement activation as assessed by their ability to induce CDC of Daudi tumor cells. All oligomerization-inhibited mutants were unable to induce CDC, with the exception of mutant C which was strongly reduced, but displayed some residual activity. However, a 1:1 mixture of complementary variants restored CDC activity comparable to the wild-type control antibody (Figure 4d,e; Supporting Information, Table S1, lists all mutants). Mutant mixtures that allowed the generation of dimers were unable to induce CDC, whereas mixtures resulting in trimers were strongly (>1.5 logs) reduced in potency (Figure 4f,g). Finally, further control mixtures of mutants allowing hexamer formation again demonstrated similar CDC compared to the control (Figure 4h). Additional controls and mirror-image mixtures were performed and showed similar results (Supporting Information, Figure S5a−g).

CDC Activation Requires at Least Four C1q Binding Sites per IgG Hexamer. The studies above indicated that IgG monomers, dimers, and trimers do not appreciably induce CDC. To address this question using a different approach and to extend the analysis to higher-order oligomers, we varied the valency of binding sites in randomly assembled IgG oligomers using mutation K322A, which is known to abrogate C1q binding and CDC activity.[35−37] When the ratio of IgG1-K322A to wild-type IgG1 was titrated, CDC efficacy was proportional to the wild-type IgG1 content (Figure 5a). Interestingly, when the observed CDC levels were normalized from 0% to 100% to fit stochastic probability functions, CDC levels were proportional to the stochastic abundance of hexamers containing four or more subunits with unmutated C1q binding sites (Figure 5b; Supporting Information, Table S2). K322A mutations were also introduced into antibodies that form defined heterohexameric arrangements (Figure 5c). Mutants containing the autoinhibitory mutation A or B, but also mixtures containing at least one mutant with an additional K322A C1q-binding knockout mutation, failed to induce cell lysis. Only heterohexamers containing wild-type C1q binding sites in all of the six subunits showed efficient CDC (Supporting Information, Figure S5h). Surprisingly, different heterohexameric assemblies containing wild-type C1q binding sites in three or four of the six subunits still failed to show appreciable CDC activity (Figure 5c,d). This suggests that up to four C1 binding sites in a hexamer are insufficient for complement activation and indicate that complement activation requires the binding of more than four C1q headpieces.

Real-Time Binding of C1q to IgG Oligomers Assembled at DNP-Labeled Lipid Bilayers. Having confirmed the dependency of complement activation on higher-order oligomers assembled on cells, we next attempted to directly visualize the binding of complement factor C1q to heterogeneous IgG oligomer distributions at SLBs by HS-AFM. We studied binding to the IgG1-DNP-E430G, as it generates a higher number of hexamers on the antigenic surface than the wild-type variant (Figure 6a), but it remains monomeric in solution. We also previously showed that the IgG1-E430 mutant, similar to wild-type, does not form any solution-phase hexamers in the presence of C1q, in stark contrast to the IgG1-RGY variant.[31] After higher oligomers/hexamers were identified (red circles), C1q (structural assessment on mica: Figure 6b,c, Movie S11) was injected into the HS-AFM's liquid chamber. C1q binding was visible through a ∼10 nm increase in height (Figure 6a, blue circles). Recording the same sample area repeatedly every 5 min revealed that C1q bound specifically and remarkably stably to higher oligomers, likely hexamers, but not to smaller oligomers or single IgGs, consistent with our measurements of CDC activity on tumor cells (Figure 4) and the activation stoichiometry studied in Figure 5.

Discussion. Upon surface-antigen binding of a single IgG, oligomerization may proceed via two different pathways: recruitment from solution and diffusion-driven lateral collisions. For preoligomerized or high-density antigens, the latter may be less important, but for low-density epitopes that exhibit limited or no self-oligomerization/clustering, oligomerization through lateral collision may contribute substantially. The lateral pathway requires monovalent antigen binding of IgG to the membrane—a configuration that can be artificially prepared and exploited in therapy by the use of functionally monovalent or bispecific IgGs. Whether both mechanisms may be employed during polyclonal IgG responses of modest

DOI: 10.1021/acs.nanolett.9b02220
Nano Lett. 2019, 19, 4787−4796

affinity or by IgG4 antibodies which are naturally bispecific in vivo[38] is presently unclear.

When we assessed the CDC potency of different intermediates along the IgG hexamerization pathway, monomeric, dimeric, and trimeric IgG assemblies did not substantially contribute to CDC potency. The apparent inconsistency with historical data may be partly explained by the use of cells with exaggerated complement sensitivity due to a lack of proper complement defense due to deficiencies in complement-regulatory factors or the use of heterologous complement. The poor CDC activity of smaller IgG oligomers is also consistent with our observation by native mass spectrometry of undetectable C1q binding to small IgG oligomers (i.e., monomers, dimers, trimers, and tetramers) assembled in solution.[31] Modulation of C1q binding site valency in hexamers suggested that the presence of four C1q binding sites in a hexamer also is insufficient for complement activation. However, an alternative explanation that we cannot exclude from our studies is that activation of C1 requires four C1q headpieces to be bound in close proximity to adjacent subunits in IgG hexamers. Both possibilities are consistent with recent cryo-EM images of C1-IgG complexes assembled in solution, which showed a distribution of complexes with four, five, or six headpieces adjacently bound to IgG hexamers[9] as well as cryo-EM on liposomes which showed the strongest resolution for four adjacent headpieces.[18] From this perspective, it can be hypothesized that the binding of only two or three adjacent hexameric Fc binding sites by C1 does not result in sufficient compaction of its C1q arms to induce the conformational arrangements that allow C1r to activate C1s.[9] Interestingly, IgM hexamers without J-chain and IgM pentamers with one J-chain adopted surprisingly similar structures, in which the J-chain replaced one "missing" subunit but preserved the otherwise hexagonal symmetry of the IgM subunits.[39] This suggests that IgG hexamers assembled on surfaces, IgM pentamers, and IgM hexamers may present similar stereochemical danger patterns recognized by C1q.

Antibodies and antibody constructs are widely used in biotechnology and nanotechnology; however, their ability to self-assemble into ordered oligomers on antigenic surfaces has not yet been much exploited. An application of Fc-dependent hexamer formation on cells is found in the targeting of (low-density) antigens, such as members of the tumor necrosis factor receptor superfamily which may be activated by receptor clustering. Thus, Zhang et al. demonstrated that mutations that increased Fc−Fc interactions led to increased clustering and agonism of the target antigen OX40.[40,41] Similarly, a mixture of two noncompeting antibodies against DR5 containing mutations which enhanced hexamer formation, currently in clinical development (NCT03576131), induced increased cytotoxicity of multiple myeloma tumor cells.[42] Finally, a mixture of two hexamerization-enhanced mutants targeting two distinct B cell lymphoma targets, CD20 and CD37, were recently shown to form heterohexamers that increased their colocalization and CDC.[43] Our data in combination with these examples suggest that molecules containing Fc domains that self-assemble into homo- or hetero-oligomers upon or during cell binding provide novel opportunities for guiding cell surface receptors into functional clusters. In oligomers assembled from bispecific antibody molecules, it is imaginable that the unbound binding arm could serve as specific binding sites for toxins, drugs, or nanoparticles which could thus be locally enriched on a target surface.[44,45] Notably, as assembly is mediated by Fc−Fc contacts, one or both antibody Fab arms in these macromolecular assemblies could be replaced by other functional (binding) moieties, such as a cytokine or receptor extracellular domain.[46] Our study therefore provides novel mechanistic insights in the dynamics of (immune) complex formation on antigenic surfaces and offers novel opportunities for antibody engineering and tool development, for optimizing monoclonal and polyclonal antibody-based therapeutics as well as vaccine design.

■ ASSOCIATED CONTENT

Supporting Information

The Supporting Information is available free of charge on the ACS Publications website at DOI: 10.1021/acs.nanolett.9b02220.

Experimental methods and additional data and figures including HS-AFM data, complement-mediated lysis assays results, molecular designs, and additional CDC results (PDF)

Movie S1: Overview scan of IgG1-DNP-WT bound to DNP-labeled SLB (AVI)

Movie S2: Overview scan of IgG1-DNP-E430G bound to DNP-labeled SLB (AVI)

Movie S3: Overview scan of IgG1-DNP-RGY bound to DNP-labeled SLB (AVI)

Movie S4: Force induced dissociation of an IgG1-DNP-RGY hexamer (AVI)

Movie S5: Force induced dissociation of an IgG1-DNP-RGY hexamer (AVI)

Movie S6: High-resolution imaging of an individual IgG1-DNP-RGY hexamer (AVI)

Movie S7: Bivalently bound IgGs on DNP-SLBs (AVI)

Movie S8: IgG1-DNP-E430G oligomerization from solution (AVI)

Movie S9: Lateral oligomerization of bsIgG1-DNP/b12-E430G on a DNP-SLB in IgG-free buffer (AVI)

Movie S10: bsIgG1-DNP/b12-E430G oligomerization from solution (AVI)

Movie S11: High speed atomic force microscopy of complement component C1q (AVI)

■ AUTHOR INFORMATION

Corresponding Author

*E-mail: johannes.preiner@fh-linz.at.

ORCID

Guanbo Wang: 0000-0002-5468-8993

Albert J. R. Heck: 0000-0002-2405-4404

Peter Hinterdorfer: 0000-0003-2583-1305

Johannes Preiner: 0000-0002-6755-6543

Author Contributions

F.J.B., J.P., Ja.S., P.H., R.N.d.J., and P.W.H.I.P. conceived the project. G.W., F.J.B., J.P., J.S., and R.N.d.J. analyzed data. F.J.B., J.P., J.S., R.N.d.J., and P.W.H.I.P. wrote the manuscript. All authors commented on the manuscript. J.P. and J.S. designed and performed HS-AFM experiments. F.J.B. and R.N.d.J. designed and performed functional complement assays. G.W. and A.J.R.H. designed and performed MS experiments.

Notes

The authors declare the following competing financial interest(s): F.J.B., R.N.d.J., Ja.S., and P.W.H.I.P. are inventors

DOI: 10.1021/acs.nanolett.9b02220
Nano Lett. 2019, 19, 4787−4796

on patent applications related to complement activation by therapeutic antibodies and own Genmab stock. J.S., G.W., and J.P. received Genmab funding.

■ ACKNOWLEDGMENTS

We thank Marleen Voorhorst for excellent technical assistance. This work was supported by the European Fund for Regional Development (EFRE, IWB2020) and the Federal State of Upper Austria. G.W. and A.J.R.H. acknowledge financial support by the large-scale proteomics facility Proteins@Work (Project 184.032.201) embedded in The Netherlands Proteomics Centre. A.J.R.H. acknowledges support from The Netherlands Organization for Scientific Research (NWO) through the Spinoza Award SPI.2017.028.

■ ABBREVIATIONS

mAb, monoclonal antibodies; SLB, supported lipid bilayer; HS-AFM, high-speed atomic force microscopy; CDC, complement-dependent cytotoxicity; IgG, immunoglobulin G; bsIgG, bispecific immunoglobulin G; HP-SEC, size exclusion chromatography; MS, native mass spectrometry

■ REFERENCES

(1) Cragg, M. S.; Morgan, S. M.; Chan, H. T. C.; Morgan, B. P.; Filatov, A. V.; Johnson, P. W. M.; French, R. R.; Glennie, M. J. Complement-Mediated Lysis by Anti-CD20 MAb Correlates with Segregation into Lipid Rafts. *Blood* **2003**, *101* (3), 1045−1052.

(2) Pawluczkowycz, A. W.; Beurskens, F. J.; Beum, P. V.; Lindorfer, M. A.; van de Winkel, J. G. J.; Parren, P. W. H. I.; Taylor, R. P. Binding of Submaximal C1q Promotes Complement-Dependent Cytotoxicity (CDC) of B Cells Opsonized with Anti-CD20 MAbs Ofatumumab (OFA) or Rituximab (RTX): Considerably Higher Levels of CDC Are Induced by OFA than by RTX. *J. Immunol.* **2009**, *183* (1), 749−758.

(3) de Weers, M.; Tai, Y.-T.; van der Veer, M. S.; Bakker, J. M.; Vink, T.; Jacobs, D. C. H.; Oomen, L. A.; Peipp, M.; Valerius, T.; Slootstra, J. W.; et al. Daratumumab, a Novel Therapeutic Human CD38 Monoclonal Antibody, Induces Killing of Multiple Myeloma and Other Hematological Tumors. *J. Immunol.* **2011**, *186* (3), 1840−1848.

(4) Teeling, J. L.; Mackus, W. J. M.; Wiegman, L. J. J. M.; van den Brakel, J. H. N.; Beers, S. A.; French, R. R.; van Meerten, T.; Ebeling, S.; Vink, T.; Slootstra, J. W.; et al. The Biological Activity of Human CD20 Monoclonal Antibodies Is Linked to Unique Epitopes on CD20. *J. Immunol.* **2006**, *177* (1), 362−371.

(5) Meng-Qi, X.; Hale, G.; Waldmann, H. Efficient Complement-Mediated Lysis of Cells Containing the CAMPATH-1 (CDw52) Antigen. *Mol. Immunol.* **1993**, *30* (12), 1089−1096.

(6) Melis, J. P. M.; Strumane, K.; Ruuls, S. R.; Beurskens, F. J.; Schuurman, J.; Parren, P. W. H. I. Complement in Therapy and Disease: Regulating the Complement System with Antibody-Based Therapeutics. *Mol. Immunol.* **2015**, *67* (2A), 117−130.

(7) Burton, D. R. Antibody: The Flexible Adaptor Molecule. *Trends Biochem. Sci.* **1990**, *15* (2), 64−69.

(8) Gaboriaud, C.; Ling, W. L.; Thielens, N. M.; Bally, I.; Rossi, V. Deciphering the Fine Details of C1 Assembly and Activation Mechanisms: "Mission Impossible"? *Front. Immunol.* **2014**, *5*, 565.

(9) Ugurlar, D.; Howes, S. C.; de Kreuk, B.-J.; Koning, R. I.; de Jong, R. N.; Beurskens, F. J.; Schuurman, J.; Koster, A. J.; Sharp, T. H.; Parren, P. W. H. I. Structures of C1-IgG1 Provide Insights into How Danger Pattern Recognition Activates Complement. *Science* **2018**, *359* (6377), 794−797.

(10) Borsos, T.; Rapp, H. J. Complement Fixation on Cell Surfaces by 19S and 7S Antibodies. *Science* **1965**, *150* (3695), 505−506.

(11) Hughes-Jones, N. C. Functional Affinity Constants of the Reaction between 125I-Labelled C1q and C1q Binders and Their Use in the Measurement of Plasma C1q Concentrations. *Immunology* **1977**, *32* (2), 191−198.

(12) Humphrey, J. H. Haemolytic Efficiency of Rabbit IgG Anti-Forssman Antibody and Its Augmentation by Anti-Rabbit IgG. *Nature* **1967**, *216* (5122), 1295−1296.

(13) Linscott, W. D. Complement Fixation: The Effects of IgG and IgM Antibody Concentration on C1-Binding Affinity. *J. Immunol.* **1970**, *105* (4), 1013−1023.

(14) Sledge, C. R.; Bing, D. H. Binding Properties of the Human Complement Protein Clq. *J. Biol. Chem.* **1973**, *248* (8), 2818−2823.

(15) Tschopp, J.; Schulthess, T.; Engel, J.; Jaton, J.-C. Antigen-Independent Activation of the First Component of Complement C1 by Chemically Crosslinked Rabbit IgG-Oligomers. *FEBS Lett.* **1980**, *112* (2), 152−154.

(16) Tschopp, J.; Villiger, W.; Lustig, A.; Jaton, J.-C.; Engel, J. Antigen-Independent Binding of IgG Dimers to C1 q as Studied by Sedimentation Equilibrium, Complement Fixation and Electron Microscopy. *Eur. J. Immunol.* **1980**, *10* (7), 529−535.

(17) Wright, J. K.; Tschopp, J.; Jaton, J. C.; Engel, J. Dimeric, Trimeric and Tetrameric Complexes of Immunoglobulin G Fix Complement. *Biochem. J.* **1980**, *187* (3), 775−780.

(18) Diebolder, C. A.; Beurskens, F. J.; de Jong, R. N.; Koning, R. I.; Strumane, K.; Lindorfer, M. A.; Voorhorst, M.; Ugurlar, D.; Rosati, S.; Heck, A. J. R.; et al. Complement Is Activated by IgG Hexamers Assembled at the Cell Surface. *Science* **2014**, *343* (6176), 1260−1263.

(19) de Jong, R. N.; Beurskens, F. J.; Verploegen, S.; Strumane, K.; van Kampen, M. D.; Voorhorst, M.; Horstman, W.; Engelberts, P. J.; Oostindie, S. C.; Wang, G.; et al. A Novel Platform for the Potentiation of Therapeutic Antibodies Based on Antigen-Dependent Formation of IgG Hexamers at the Cell Surface. *PLoS Biol.* **2016**, *14* (1), No. e1002344.

(20) Ando, T.; Kodera, N.; Takai, E.; Maruyama, D.; Saito, K.; Toda, A. A High-Speed Atomic Force Microscope for Studying Biological Macromolecules. *Proc. Natl. Acad. Sci. U. S. A.* **2001**, *98* (22), 12468−12472.

(21) Kodera, N.; Yamamoto, D.; Ishikawa, R.; Ando, T. Video Imaging of Walking Myosin V by High-Speed Atomic Force Microscopy. *Nature* **2010**, *468* (7320), 72−76.

(22) Uchihashi, T.; Iino, R.; Ando, T.; Noji, H. High-Speed Atomic Force Microscopy Reveals Rotary Catalysis of Rotorless F1-ATPase. *Science* **2011**, *333* (6043), 755.

(23) Casuso, I.; Khao, J.; Chami, M.; Paul-Gilloteaux, P.; Husain, M.; Duneau, J. P.; Stahlberg, H.; Sturgis, J. N.; Scheuring, S. Characterization of the Motion of Membrane Proteins Using High-Speed Atomic Force Microscopy. *Nat. Nanotechnol.* **2012**, *7* (8), 525−529.

(24) Preiner, J.; Horner, A.; Karner, A.; Ollinger, N.; Siligan, C.; Pohl, P.; Hinterdorfer, P. High-Speed AFM Images of Thermal Motion Provide Stiffness Map of Interfacial Membrane Protein Moieties. *Nano Lett.* **2015**, *15* (1), 759−763.

(25) Karner, A.; Nimmervoll, B.; Plochberger, B.; Klotzsch, E.; Horner, A.; Knyazev, D. G.; Kuttner, R.; Winkler, K.; Winter, L.; Siligan, C.; et al. Tuning Membrane Protein Mobility by Confinement into Nanodomains. *Nat. Nanotechnol.* **2017**, *12* (3), 260−266.

(26) Shibata, M.; Yamashita, H.; Uchihashi, T.; Kandori, H.; Ando, T. High-Speed Atomic Force Microscopy Shows Dynamic Molecular Processes in Photoactivated Bacteriorhodopsin. *Nat. Nanotechnol.* **2010**, *5* (3), 208−212.

(27) Fantner, G. E.; Barbero, R. J.; Gray, D. S.; Belcher, A. M. Kinetics of Antimicrobial Peptide Activity Measured on Individual Bacterial Cells Using High-Speed Atomic Force Microscopy. *Nat. Nanotechnol.* **2010**, *5* (4), 280−285.

(28) Shibata, M.; Uchihashi, T.; Ando, T.; Yasuda, R. Long-Tip High-Speed Atomic Force Microscopy for Nanometer-Scale Imaging in Live Cells. *Sci. Rep.* **2015**, *5*, 8724.

(29) Colom, A.; Casuso, I.; Rico, F.; Scheuring, S. A Hybrid High-Speed Atomic Force−Optical Microscope for Visualizing Single Membrane Proteins on Eukaryotic Cells. *Nat. Commun.* **2013**, *4*, 2155.

DOI: 10.1021/acs.nanolett.9b02220
Nano Lett. 2019, 19, 4787−4796

(30) Preiner, J.; Kodera, N.; Tang, J.; Ebner, A.; Brameshuber, M.; Blaas, D.; Gelbmann, N.; Gruber, H. J.; Ando, T.; Hinterdorfer, P. IgGs Are Made for Walking on Bacterial and Viral Surfaces. *Nat. Commun.* **2014**, *5*, 4394.
(31) Wang, G.; de Jong, R. N.; van den Bremer, E. T. J.; Beurskens, F. J.; Labrijn, A. F.; Ugurlar, D.; Gros, P.; Schuurman, J.; Parren, P. W. H. I.; Heck, A. J. R. Molecular Basis of Assembly and Activation of Complement Component C1 in Complex with Immunoglobulin G1 and Antigen. *Mol. Cell* **2016**, *63* (1), 135−145.
(32) Saphire, E. O.; Parren, P. W. H. I.; Pantophlet, R.; Zwick, M. B.; Morris, G. M.; Rudd, P. M.; Dwek, R. A.; Stanfield, R. L.; Burton, D. R.; Wilson, I. A. Crystal Structure of a Neutralizing Human IgG Against HIV-1: A Template for Vaccine Design. *Science* **2001**, *293* (5532), 1155−1159.
(33) van den Bremer, E. T.; Beurskens, F. J.; Voorhorst, M.; Engelberts, P. J.; de Jong, R. N.; van der Boom, B. G.; Cook, E. M.; Lindorfer, M. A.; Taylor, R. P.; van Berkel, P. H.; et al. Human IgG Is Produced in a Pro-Form That Requires Clipping of C-Terminal Lysines for Maximal Complement Activation. *mAbs* **2015**, *7* (4), 672−680.
(34) Labrijn, A. F.; Meesters, J. I.; de Goeij, B. E.; van den Bremer, E. T.; Neijssen, J.; van Kampen, M. D.; Strumane, K.; Verploegen, S.; Kundu, A.; Gramer, M. J.; et al. Efficient Generation of Stable Bispecific IgG1 by Controlled Fab-Arm Exchange. *Proc. Natl. Acad. Sci. U. S. A.* **2013**, *110* (13), 5145−5150.
(35) Duncan, A. R.; Winter, G. The Binding Site for C1q on IgG. *Nature* **1988**, *332* (6166), 738−740.
(36) Idusogie, E. E.; Presta, L. G.; Gazzano-Santoro, H.; Totpal, K.; Wong, P. Y.; Ultsch, M.; Meng, Y. G.; Mulkerrin, M. G. Mapping of the C1q Binding Site on Rituxan, a Chimeric Antibody with a Human IgG1 Fc. *J. Immunol.* **2000**, *164* (8), 4178−4184.
(37) Thommesen, J. E.; Michaelsen, T. E.; Løset, G. Å.; Sandlie, I.; Brekke, O. H. Lysine 322 in the Human IgG3 CH2 Domain Is Crucial for Antibody Dependent Complement Activation. *Mol. Immunol.* **2000**, *37* (16), 995−1004.
(38) van der Neut Kolfschoten, M.; Schuurman, J.; Losen, M.; Bleeker, W. K.; Martínez-Martínez, P.; Vermeulen, E.; den Bleker, T. H.; Wiegman, L.; Vink, T.; Aarden, L. A.; et al. Anti-Inflammatory Activity of Human IgG4 Antibodies by Dynamic Fab Arm Exchange. *Science* **2007**, *317* (5844), 1554−1557.
(39) Hiramoto, E.; Tsutsumi, A.; Suzuki, R.; Matsuoka, S.; Arai, S.; Kikkawa, M.; Miyazaki, T. The IgM Pentamer Is an Asymmetric Pentagon with an Open Groove That Binds the AIM Protein. *Sci. Adv.* **2018**, *4* (10), No. eaau1199.
(40) Zhang, D.; Goldberg, M. V.; Chiu, M. L. Fc Engineering Approaches to Enhance the Agonism and Effector Functions of an Anti-OX40 Antibody. *J. Biol. Chem.* **2016**, *291* (53), 27134−27146.
(41) Zhang, D.; Armstrong, A. A.; Tam, S. H.; McCarthy, S. G.; Luo, J.; Gilliland, G. L.; Chiu, M. L. Functional Optimization of Agonistic Antibodies to OX40 Receptor with Novel Fc Mutations to Promote Antibody Multimerization. *mAbs* **2017**, *9* (7), 1129−1142.
(42) van der Horst, H. J.; Overdijk, M. B.; Breij, E. C.; Chamuleau, M.; Lokhorst, H. M.; Mutis, T. Potent Ex Vivo Anti-Tumor Activity in Relapsed Refractory Multiple Myeloma Using Novel DR5-Specific Antibodies with Enhanced Capacity to Form Hexamers upon Target Binding. *Blood* **2017**, *130* (S1), 1835−1835.
(43) Oostindie, S. C.; van derHorst, H. J.; Lindorfer, M. A.; Cook, E. M.; Tupitza, J. C.; Zent, C. S.; Burack, R.; VanDerMeid, K. R.; Strumane, K.; Chamuleau, M. E. D.; et al. CD20 and CD37 Antibodies Synergize to Activate Complement by Fc-Mediated Clustering. *Haematologica* **2019**, 207266.
(44) Metz, S.; Haas, A. K.; Daub, K.; Croasdale, R.; Stracke, J.; Lau, W.; Georges, G.; Josel, H.-P.; Dziadek, S.; Hopfner, K.-P.; et al. Bispecific Digoxigenin-Binding Antibodies for Targeted Payload Delivery. *Proc. Natl. Acad. Sci. U. S. A.* **2011**, *108* (20), 8194−8199.
(45) MacDiarmid, J. A.; Mugridge, N. B.; Weiss, J. C.; Phillips, L.; Burn, A. L.; Paulin, R. P.; Haasdyk, J. E.; Dickson, K.-A.; Brahmbhatt, V. N.; Pattison, S. T.; et al. Bacterially Derived 400 Nm Particles for Encapsulation and Cancer Cell Targeting of Chemotherapeutics. *Cancer Cell* **2007**, *11* (5), 431−445.
(46) Lan, Y.; Zhang, D.; Xu, C.; Hance, K. W.; Marelli, B.; Qi, J.; Yu, H.; Qin, G.; Sircar, A.; Hernández, V. M.; et al. Enhanced Preclinical Antitumor Activity of M7824, a Bifunctional Fusion Protein Simultaneously Targeting PD-L1 and TGF-*β*. *Sci. Transl. Med.* **2018**, *10* (424), No. eaan5488.

DOI: 10.1021/acs.nanolett.9b02220
Nano Lett. 2019, 19, 4787−4796